

# IDŐJÁRÁS

*Quarterly Journal of the Hungarian Meteorological Service  
Vol. 112, No. 3–4, July–December 2008, pp. 285–300*

## **Regional photochemical model calculations for Europe concerning ozone levels in a changing climate**

**B. C. Krüger<sup>1\*</sup>, E. Katragkou<sup>2</sup>, I. Tegoulas<sup>3</sup>, P. Zanis<sup>3</sup>, D. Melas<sup>2</sup>,  
E. Coppola<sup>4</sup>, S. Rauscher<sup>4</sup>, P. Huszar<sup>5</sup> and T. Halenka<sup>5</sup>**

<sup>1</sup>*Institute of Meteorology (BOKU-Met), University of Natural Resources and Applied Life Sciences, Peter-Jordan-Str. 82, A-1190 Vienna, Austria*

<sup>2</sup>*Laboratory of Atmospheric Physics, Aristotle University of Thessaloniki (AUTH), Greece*

<sup>3</sup>*Department of Meteorology and Climatology, Aristotle University of Thessaloniki, Greece*

<sup>4</sup>*Earth System Physics Section, The Abdus Salam International Centre for Theoretical Physics (ICTP), Trieste, Italy*

<sup>5</sup>*Department of Meteorology and Environmental Protection, Charles University (CUNI), Prague, Czech Republic*

*(Manuscript received in final form October 14, 2008)*

**Abstract**—Regional photochemical model calculations were performed for three decadal time periods: 1991–2000, 2041–2050, and 2091–2100 under changing climate conditions for Europe. While the climatic conditions changed between the decades, all other input fields of the chemical model were held constant in order to separate climate effects from others. In particular, model results for summer ozone concentrations were investigated. These show increasing ozone values in response to higher temperatures and net radiation associated with increases in anthropogenic greenhouse gases. The increase of ozone is stronger in the second half of the 21st century than in the first half. In the course of the whole century, the average summer ozone maxima will rise by several ppbv over most parts of Europe with the highest change in the northwest of the continent. This increase suggests more frequent concentrations above legal thresholds in the future and is partly caused by higher emissions of biogenic hydrocarbons in the model calculation.

*Key-words:* photochemical transport model, tropospheric ozone, climate change, CECILIA project, ozone threshold level

### ***1. Introduction***

High ozone levels above legal thresholds affecting human health as well as vegetation are of primary interest in air quality research. Several factors affect

---

\* Corresponding author; E-mail: bernd.krueger@boku.ac.at

ozone concentration, including the availability of ozone precursors, namely nitrogen oxides and volatile hydrocarbons, which are to a large fraction of anthropogenic origin. In addition, ozone formation is favored under certain meteorological conditions. Therefore, the question arises, what influence climate change will have in the future on the potential of ozone formation. Ozone concentration is in part controlled by the global background level formed by the long-range transport of pollutants and the exchange of air masses between the troposphere and stratosphere as the main mechanisms. However, over populated areas, anthropogenic emissions on local and regional scales often lead to high ozone concentration levels. Therefore, projections for future burdens of ozone should be made on a regional scale, at least.

Recently, there have been several studies with regional model calculations for Europe concerning air pollution under changing climate conditions. For example, *Meleux et al.* (2007) investigated summer ozone amounts over Europe with a 50 km resolution model by comparing two time slices of 30 years each, namely 1961–1990 and 2071–2100. *Forkel and Knoche* (2007) used a nested regional climate-chemistry model with a highest spatial resolution of 20 km over central Europe and compared the two time slices of 1991–2000 and 2030–2039. *Hedegaard et al.* (2008) had a resolution of 150 km in their model and inspected three decades (1990s, 2040s, and 2090s) for the Northern Hemisphere. In all of these studies, the anthropogenic emissions were kept unchanged for the future projections, so that their focus was on the effects of changing meteorological conditions. This approach is also applied in the present study.

This work was carried out within the European FP6 project CECILIA (Central and Eastern Europe Climate Change Impact and Vulnerability Assessment, <http://www.cecilia-eu.org/>). In this project, regional climate simulations with high spatial resolution are carried out for the target area. In addition, impact studies concerning hydrology, agriculture and forestry, as well as air quality are performed. For the latter, the model runs described in this study will be used to provide boundary concentrations for photochemical model calculations with 10 km resolution in smaller regional grids within the target area of this project. Three decadal time slices, namely 1991–2000, 2041–2050, and 2091–2100 were calculated.

It is not the purpose of this study to predict exact levels of air quality of the future until the year 2100, as there are too many unknown parameters such as the amount and composition of future anthropogenic emissions of air pollutants due to progress in technology as well as changes in land use. The latter is important, since it affects the distribution and amount of biogenic and anthropogenic emissions, and it is subject of man-made changes as well as of feedbacks from climate change. Similar to the studies by the other authors mentioned above, this study was performed to investigate the effect of climate change on ozone concentrations under the assumption that all parameters affecting air quality, except for the meteorological data, are kept unchanged.

## 2. Description of the models and input data

### 2.1. RegCM and CAMx

Meteorological input files for the photochemical model were taken from a transient climate run with the hydrostatic RegCM3 model (*Pal et al.*, 2007) performed at ICTP, that was driven at the lateral boundaries by the global ECHAM5 model under forcing from the SRES-A1B IPCC greenhouse gas scenario (*Nakicenovic et al.*, 2000) for the future projections. The spatial resolution of the model was 25 km  $\times$  25 km. A part of these calculations was performed for the EU-FP6 project ENSEMBLES (<http://ensembles-eu.metoffice.com/>).

The Comprehensive Air quality Model with eXtensions (CAMx), which is available at <http://www.camx.com>, from ENVIRON International Corporation (Novato, California) is an Eulerian photochemical dispersion model that allows for regional integrated “one-atmosphere” assessments of gaseous and particulate air pollution. Model version 4.40 was used (*ENVIRON*, 2006). The chemistry mechanism invoked was an extended Carbon Bond version 4 mechanism (*Gery et al.*, 1989). This mechanism includes 117 reactions – 11 of which are photolytic – and up to 67 species (37 state gases, up to 18 state particulates and 12 radicals).

The spatial resolution of the CAMx model grid was 50 km  $\times$  50 km and the domain had 94  $\times$  102 grid cells. The domain’s vertical profile contained 12 layers with varying thicknesses, extending up to 450 hPa. The 25 km RegCM results were upscaled to this resolution by averaging. The domains of the two models were the same. The grid covered most of Europe and parts of northern Africa as it may be seen in the figures, which display the whole domain. Time resolution of meteorological input was 6 hours, the emission input as well as the output of the photochemical model had a resolution of one hour.

The RegCM output was transformed to the format required by CAMx by a pre-processor program. Some of the fields could be taken directly like wind direction, wind speed, and temperature, while others had to be calculated analytically. The vertical diffusion coefficient needed by CAMx to model the vertical transport was calculated following the method by *O’Brian* (1970). In the pre-processing step, the biogenic emissions of isoprene and monoterpenes were calculated following *Guenther et al.* (1993) with respect to the actual meteorological fields of the day from RegCM. Also the temporal disaggregation of the anthropogenic emissions was performed in the preprocessing.

Although chemical transport models usually need a relatively small spin-up time of a few days for initialization, we calculated the full year prior to the decades considered (i.e., 1990, 2040, and 2090). In addition, we ran the period from 1990 to 2001 with RegCM fields driven by the ERA-40 reanalysis (*Uppala et al.*, 2005) for the validation of the model system. The comparison of the ERA-40 run with measurements and with the control run showed a reasonable agreement and will be described in a separate study.

## 2.2. Emissions

Anthropogenic emissions used in this study are based on the UNECE/EMEP database (<http://webdab.emep.int/>) for European emissions (*Vestreng et al.*, 2005) for the year 2000. The “expert emissions” are derived from the national totals reported by the individual countries and have been completed and corrected/substituted for the use of dispersion modeling. These data comprise the annual sums of the emissions of NO<sub>x</sub>, CO, non-methane hydrocarbons, SO<sub>2</sub>, NH<sub>3</sub>, fine particles (<2.5 μm), and coarse particles (2.5 μm to 10 μm) on a 50 km × 50 km grid. 11 sectors of anthropogenic activity are distinguished.

For the Pannonean countries Austria, Czech Republic, Hungary, and Slovakia, the EMEP data for the year 2000 are downscaled to a spatial resolution of 5 km × 5 km. An emission inventory for these countries from the year 1995 (*Winiwarter and Zueger*, 1996) is used as database for the spatial distribution of the emissions within the 50 km × 50 km EMEP grid cells.

For every sector the emission model applies different distributions for the month, day of the week, and hour of the day for temporal disaggregation. The disaggregation factors are taken from the inventory by *Winiwarter and Zueger* (1996). They are available for the Pannonean countries. For all other countries the disaggregation data for Austria have been used.

The emissions from the inventories must be splitted sector specifically into the speciation of the chemical compounds that corresponds to the chemical mechanisms of the photochemical model. In the case of NO<sub>x</sub> it is assumed in all sectors of anthropogenic emissions, that 10% are NO<sub>2</sub> and 90% are NO (in molar percentages). The emissions of non-methane hydrocarbons are disaggregated in accordance with the needs of the chemical mechanism CBM-IV (*Gery et al.*, 1989). This results in specific emissions of the following species, given in CBM-IV notation: PAR (alkane groups), ETH (ethene), OLE (alcene groups), TOL and XYL (aromatics of different reactivity), FORM (formaldehyde), and ALD2 (aldehydes, ketones). The emissions of PM<sub>2.5</sub> were splitted into organic aerosol (POA), elementary carbon (PEC), and remaining aerosol following the split suggested in the EMEP model (*Simpson et al.*, 2003). In addition, the following species are emitted without chemical disaggregation: CO, SO<sub>2</sub>, NH<sub>3</sub>, and PM<sub>2.5-10</sub>.

The anthropogenic emissions were not changed between the three decades, although it may be assumed for sure, that changes, mainly in energy supply, both for stationary and mobile sources, will have the most important impact on future air quality. However, there is a large uncertainty about the actual future emissions, even for the next approaching decades, that depends on technical development and energy availability in the future.

## 2.3. Other input data

Regional photochemical transport models need concentrations of trace species prescribed at the lateral boundaries and the top of the model. They have an

influence on the model results when the wind moves air masses from the boundaries into the model. In the calculations described in this study, we assumed clean air conditions at all boundaries, namely 40 ppbv of ozone and very low mixing ratios for all other compounds. This implies that changes of these concentrations in the global background, that may be caused by changes of climate or other conditions, are not covered by this study. In addition, impacts from potential changes in stratosphere/troposphere exchange as well as effects of long range transport of pollutants, which often takes place at tropospheric altitudes above the top of our model grid (*Trickl et al.*, 2003), are not considered here. As stated previously, future changes in land use may also be expected. Such changes might affect atmospheric composition through emissions, including biogenics, and through deposition of compounds. For this parameter also the same data for the present time were used for every decade. The data come along with the preprocessor terrain of the regional mesoscale model MM5 (<http://www.mmm.ucar.edu/mm5/>). They distinguish 25 land use categories and are based on global data from the United States Geological Survey (USGS).

### 3. Results

#### 3.1. Daily maxima of ozone in summer

In air quality studies, changes in the daily maximum concentration of ozone are of particular interest, since they allow us to estimate to which extent legal thresholds of ozone may be exceeded in a future climate. At present, following European legislation, the population has to be informed about ozone volume mixing ratios exceeding 90 ppbv. Values above 120 ppbv must lead to further measures.

However, it must be noted that the spatial resolution of the model setup in this study does not allow calculating urban plumes. Instead, only background concentrations are calculated. Therefore, the calculated maxima are expected to be lower than the maxima typically measured. Averaging may also result in lower values than it may be observed in the real world. In the following, seasonal averages of the daily maxima for the decades considered during summer are presented.

Seasonal averages of the daily ozone maxima as calculated for the control decade 1991–2000 for summer (JJA) are displayed in *Fig. 1* (upper left panel). The highest values of more than 60 ppbv are obtained over the Mediterranean Sea. A latitudinal gradient can be observed with the lowest values in the north, and the highest values in the south. In general, this corresponds to the observed behavior of ozone over Europe at the present time.

The upper right panel of *Fig. 1* shows the difference in the decadal average of the daily ozone maxima between the mid-century period and the control run. All differences are small. An increase below 2.5 ppbv can be observed over the

southeast part of Europe, stretching as far west as Italy and southern Germany. For most of the rest of the model domain over Europe, a slight decrease of the ozone maxima occurs. In a belt from southern England along the North Sea coast to southern Scandinavia, this decrease is somewhat stronger, but still below 5 ppbv.

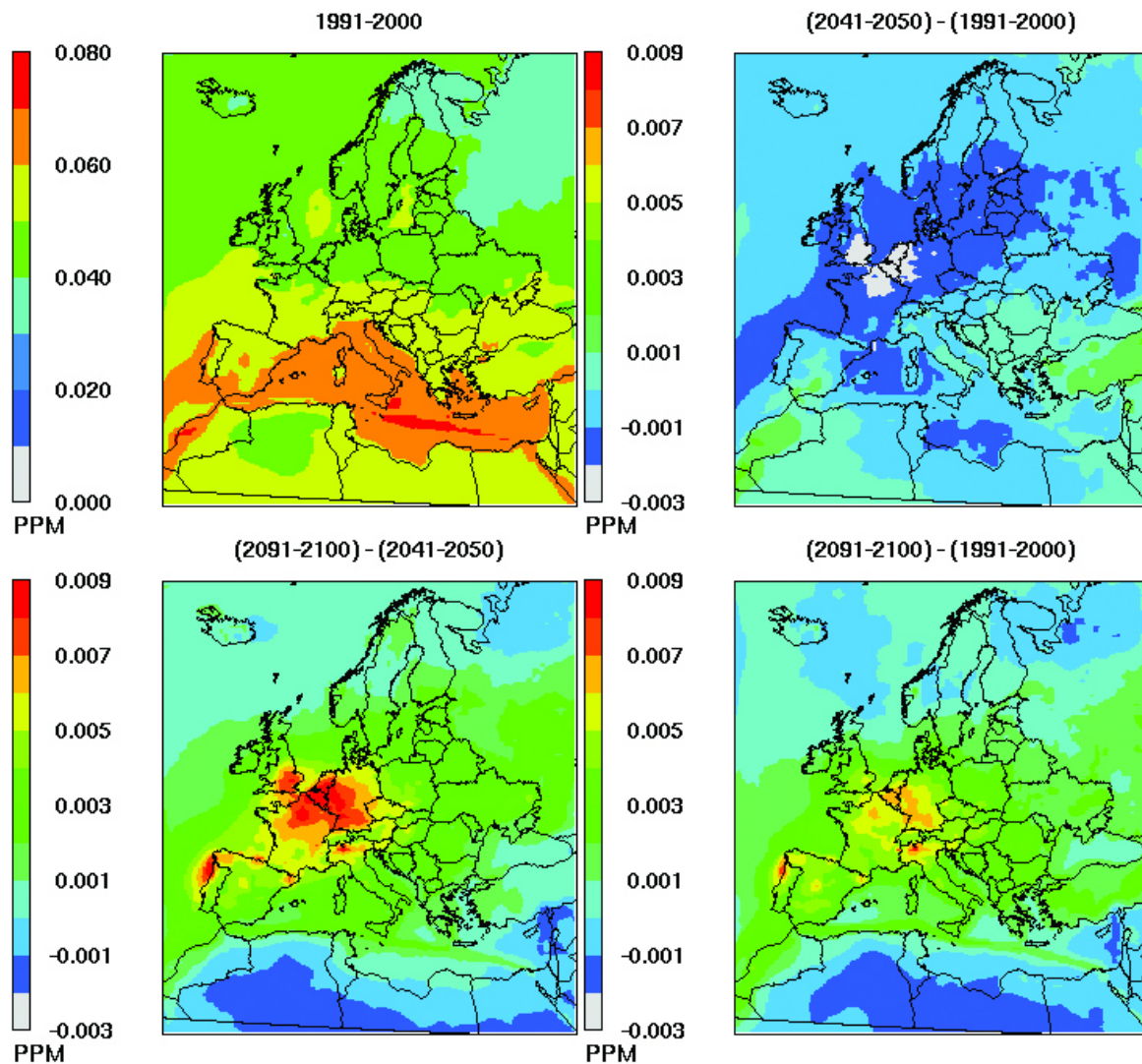


*Fig. 1.* Average of the daily maxima of ozone volume mixing ratio in summer (JJA) from the control decade 1991–2000 (upper left), and differences of the maximum ozone volume mixing ratios in summer between the calculated decades: first half-century (upper right), second half-century (lower left), and whole century (lower right).

Between the mid-century and end-century decades, a much stronger increase of the ozone maxima occurs. The highest increase is located over southern England, northern France, the Benelux countries, and western Germany reaching about 10 ppbv. However, with the exception of Africa, the eastern Mediterranean, and northern Russia, an increase of ozone is calculated all over the model domain.

The difference between the results of the end-century and control runs showing the development of the ozone maxima within 100 years is displayed in the lower right panel of *Fig. 1*. Due to the stronger increase in the second half of the 21st century, the decrease of ozone in the first half over wide parts of Europe is compensated. The highest change occurs over northern France, Belgium, and western Germany, as well as over the Po valley in Italy. These regions have the highest emissions of ozone precursors at the present time. Since the anthropogenic emissions were not changed between the decades, this emission pattern persists throughout the century.

### 3.2. Daily maxima of ozone in other seasons

In the other seasons the averaged daily maxima of ozone do not change as strongly as in summer. In spring (MAM) the ozone values increase from the control decade to the end-century decade by about 3 ppbv over most parts of Europe except for Scandinavia and the British Isles, where the increase is lower or even a slight decrease was calculated. The spring increase is of the same amount as in summer, except for those parts of western Europe that show a stronger summer increase. As an illustration, *Fig. 2* displays the change during the whole century in spring and autumn.

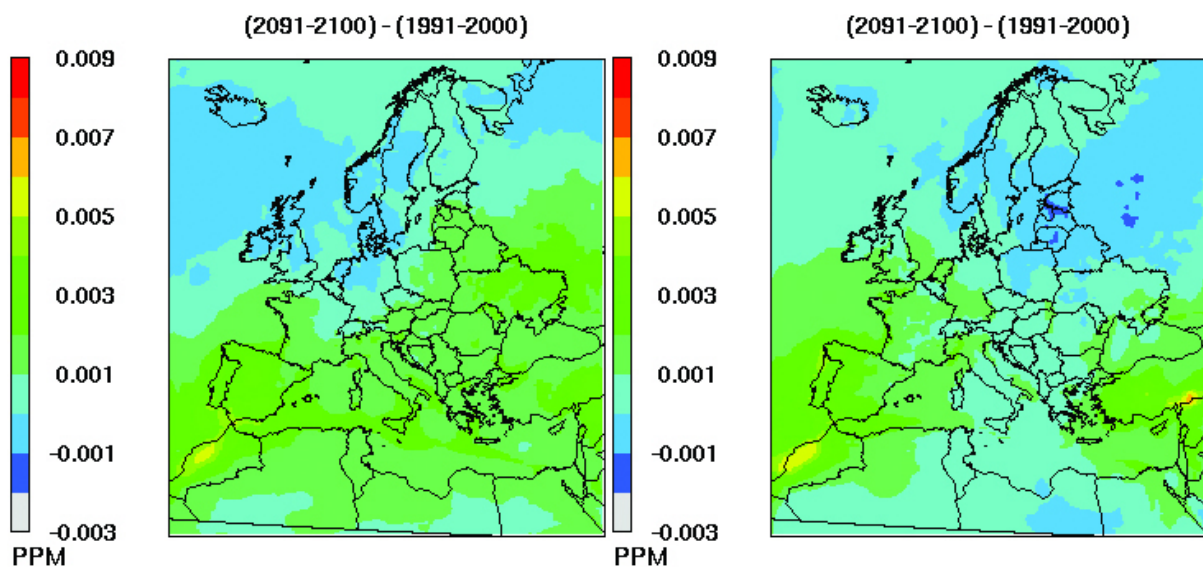


*Fig. 2.* Differences of the average daily maxima of ozone volume mixing ratio in spring (MAM, left) and autumn (SON, right) during the whole century.

In autumn (SON) the average of the daily ozone maxima decreases over most of Europe in the first half of the 21st century and increases in the second half; each change is approximately 3 ppbv. For the whole century this results in a slightly stronger increase over western Europe than over the central and eastern regions. Winter (DJF) shows the smallest changes. In contrast to the

other seasons, a decrease of ozone occurs in winter in the second half of the century in most land-covered parts of the model domain, while other regions show a small increase between the control decade and the mid-century decade.

Since the highest concentrations of ozone occur in summer causing perturbations of the air quality by exceeding legal thresholds, and since the highest alterations due to climate change in these calculations also occur in summer, in the following only the changes in summer will be further considered in this study.

### 3.3. AOT40

Accumulated ozone exposure values over a certain threshold (AOT) are common measures for the ozone impact. In this study we compare AOT40 (accumulated ozone over a threshold of 40 ppbv) for the period from April to September, which is considered as a measure for the impact of ozone on forests. The sum of the differences between the hourly mean ozone concentration (in ppb) and 40 ppb for each hour when the concentration exceeds 40 ppb, accumulated between 8:00 and 20:00 hours during the period is calculated. As a long-term objective for the protection of forests, a maximum value of 10000 ppbv h is considered. (*European Communities, 2002*).

The upper left panel of *Fig. 3* shows the average AOT40 data as they were calculated for the control period 1991–2000. Only in northern Europe the long-term objective is not exceeded. The highest values can be found over the Mediterranean Sea. In the first half of the 21st century, AOT 40 goes down over most of Europe, except of the Iberian Peninsula and southeast Europe (upper right panel), while there is a strong increase over most of Europe in the second half of the century (lower left panel). The lower right panel shows that during the whole 21st century, AOT40 values will go up over the whole of Europe with the highest increase over the Iberian Peninsula and the Alps.

Similar results were obtained for other quantities describing the exposure to elevated ozone concentrations like AOT40 (May–July), which is considered as a measure for the exposure of agricultural plants during the growing period, or AOT60, which measures the exposure of humans. Also average ozone concentrations show a small change during the first half of the 21st century and a strong increase in the second half, with stronger increases in the south part of Europe than in the north.

### 3.4. Temperature

As an indicator for the changing climate, the changes of the temperature in the lowest model level are shown, as they were taken from the RegCM results, which were input data to the photochemical model CAMx. The upper left panel of *Fig. 4* shows the average summer temperature from the control period 1991–2000 with the expected north-south gradient.

The changes in average temperature until the mid-century decade 2041–2050 are less than 1 degree over most of Europe except for the very northern areas as well as southern Spain, Sicily, and southern Greece, where an increase between 1 and 2 degrees occurs, as it is shown in the upper right panel. Over England and northwestern France there is even a decrease of the average temperature. In the second half of the 21st century a much stronger increase occurs, displayed in the lower left panel, amounting to 1 to 2 degrees in northern Europe, up to 3 degrees in Germany and eastern Europe, up to 4 degrees over France and Italy, and even more over the Iberian peninsula.

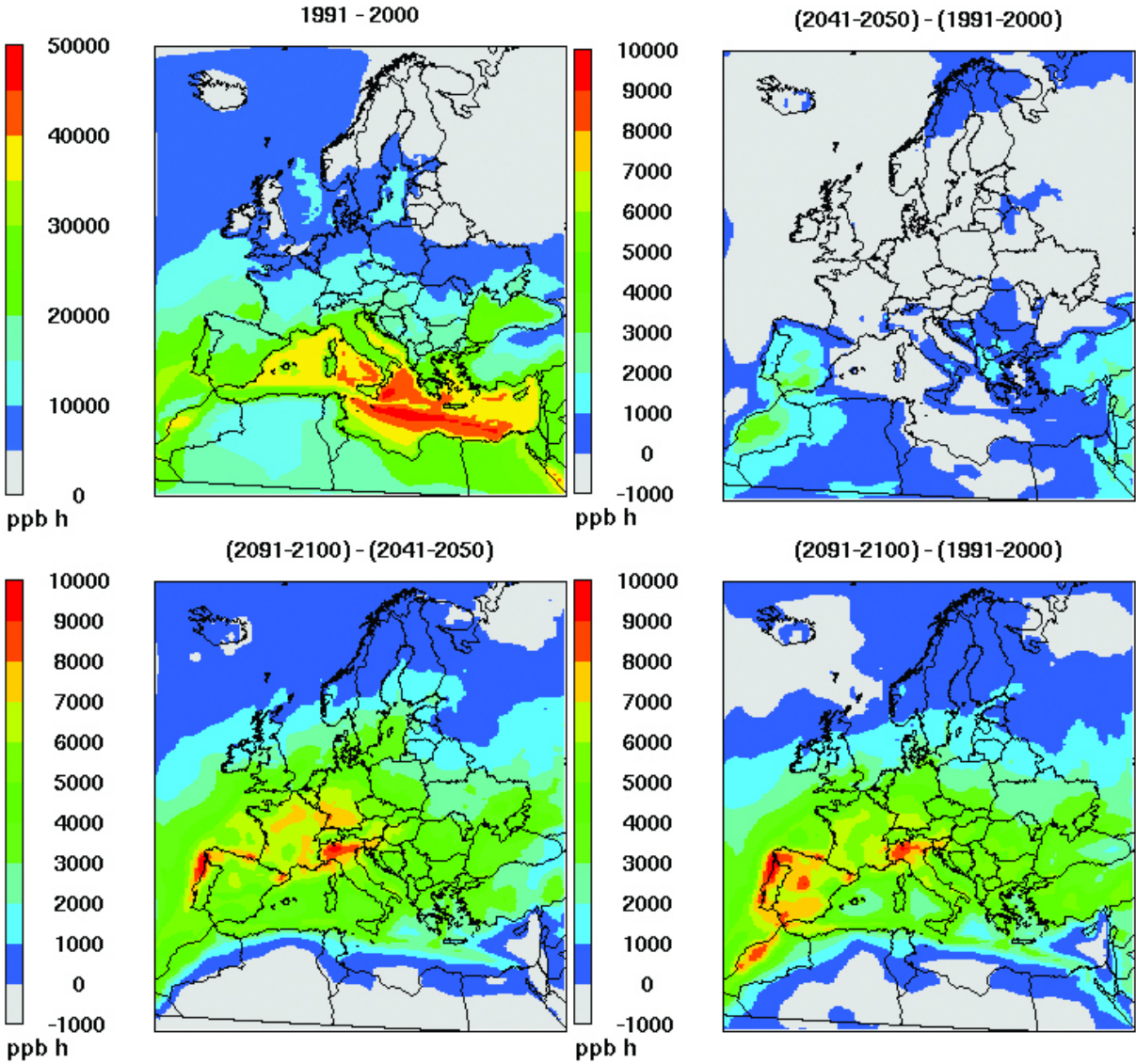


Fig 3. AOT40 (accumulated ozone over a threshold of 40 ppbv) from April to September in the control decade 1991–2000 (upper left), and differences of AOT40 from April to September between the calculated decades: first half-century (upper right), second half-century (lower left), and whole century (lower right).

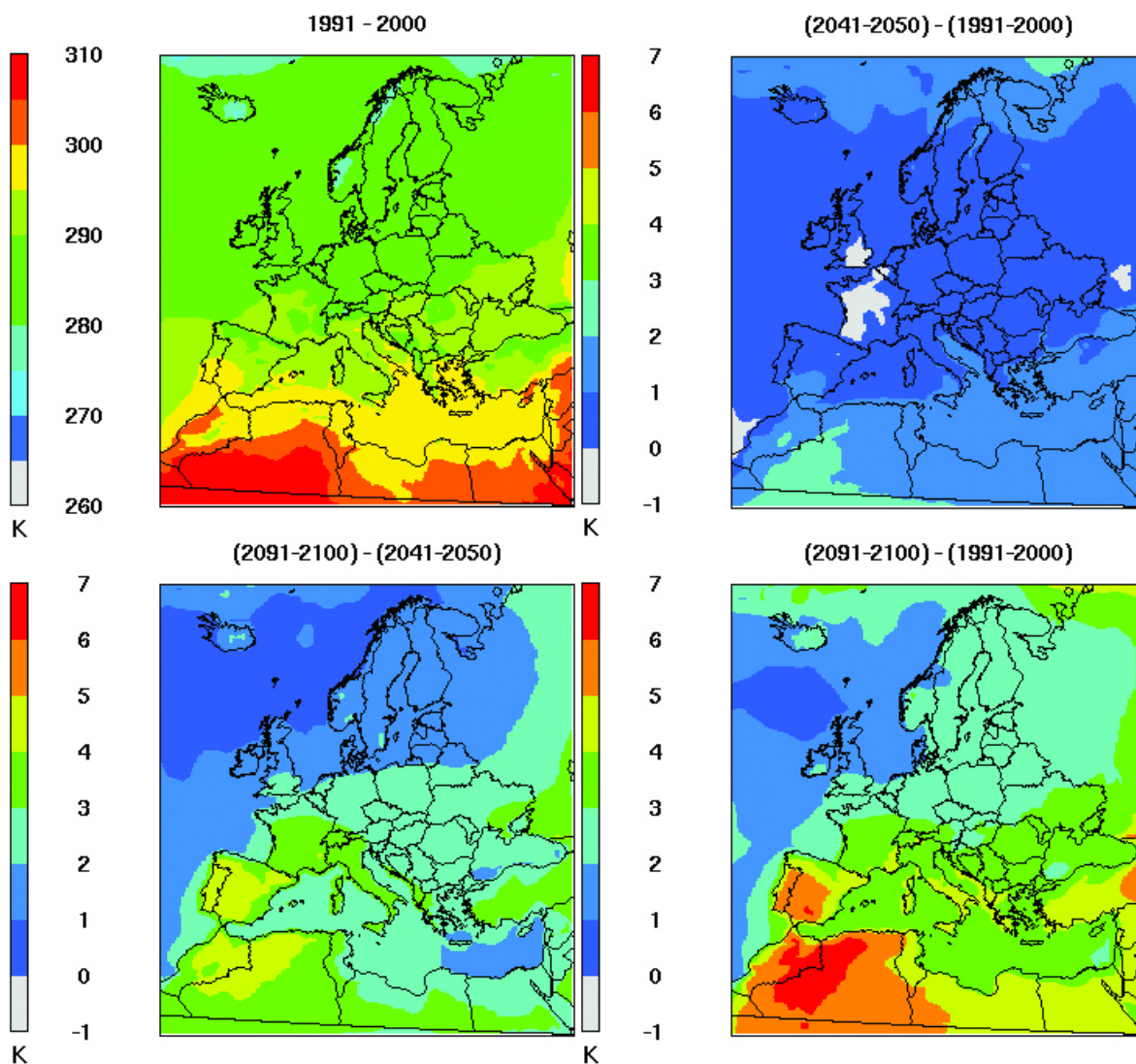


Fig. 4. Average temperature in the lowest model level in summer (JJA) in the control decade 1991–2000 (upper left), and differences of the average temperatures in summer between the calculated decades: first half-century (upper right), second half-century (lower left), and whole century (lower right).

### 3.5. Cloud optical depth

Besides temperature, photochemical activity is strongly influenced by the amount of radiation, which drives the formation of radicals and enhances the production of biogenic hydrocarbons. These emissions act as precursors in ozone formation along with the anthropogenic emissions of hydrocarbons and nitrogen oxides. In CAMx the photolysis rates are calculated from a look-up table that contains clear sky photolysis rates at various solar zenith angles, altitudes, total ozone columns, values for the surface albedo, and atmospheric turbidity. The effect of clouds is treated based upon the RADM approach (*Chang et al.*, 1987), in which the cloud optical depth is used to scale down the photolysis rates for layers within or below clouds to account for UV attenuation, or to scale up the rates for layers above clouds to account for UV reflection. The

cloud optical depth is calculated by an empirical expression with the preprocessor from the actual cloud water mixing ratio.

As a qualitative measure of the attenuation of radiation, *Fig. 5* shows the average cloud optical depth of the control period (upper left panel) during summer. The highest values in the model domain occur over the Atlantic Ocean, and the lowest values are observed over the Mediterranean Sea. During the first half of the 21st century there is an increase all over Europe. The highest rise occurs over the sea (Atlantic Ocean, North Sea, Baltic Sea), while over southern Europe the increase is small (upper right panel). This increase in the cloud optical depth leads to a reduction in photochemically active radiation.

In the second half of the century the cloud optical depth decreases all over Europe. With the exception of northern Europe, this decrease compensates the increase in the first half (lower right panel). This net effect is that the photochemically active radiation becomes stronger.

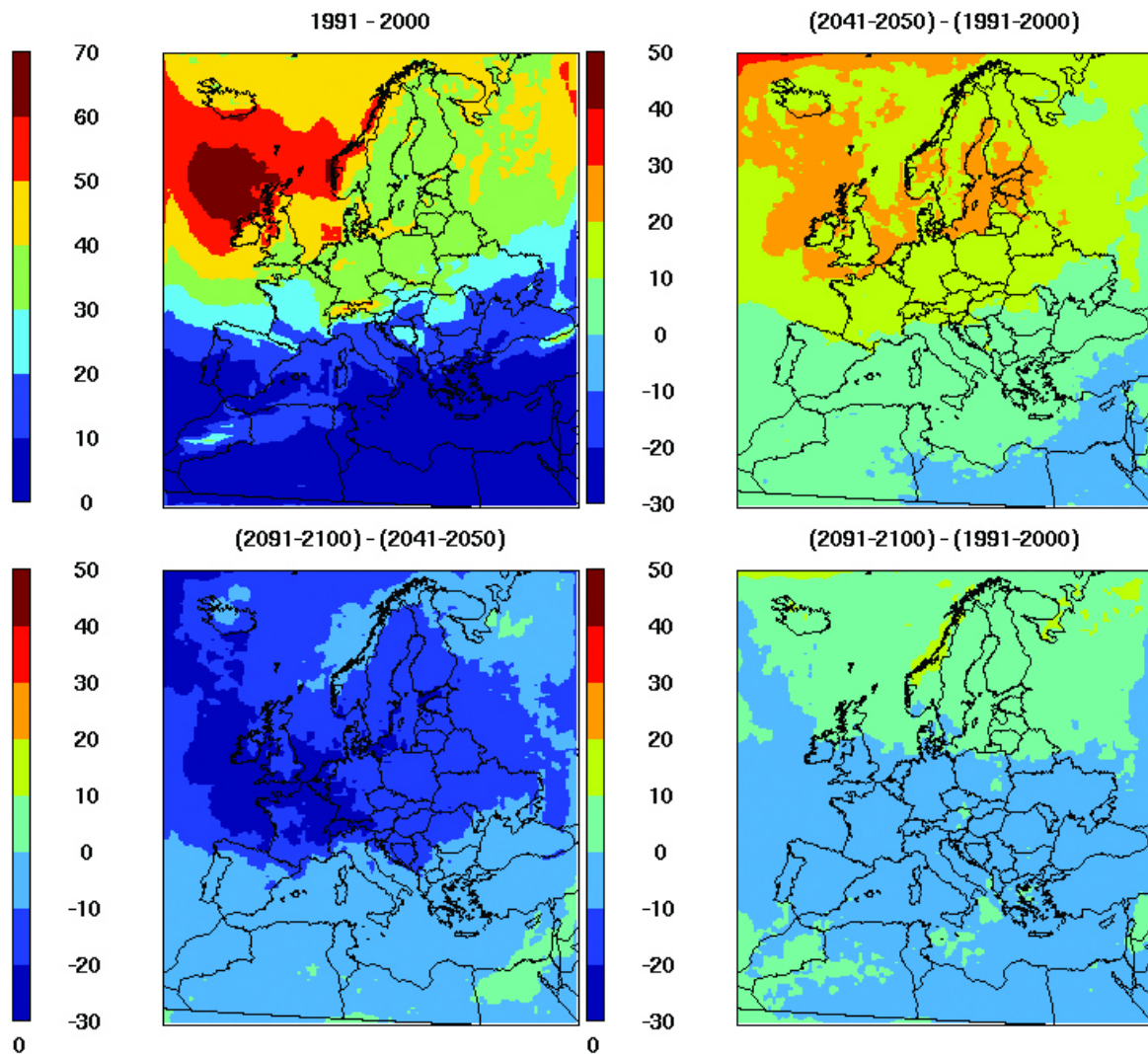


*Fig. 5.* Average cloud optical depth in the lowest model level in summer (JJA) in the control decade 1991–2000 (upper left), and differences of the average cloud optical depths in summer between the calculated decades: first half-century (upper right), second half-century (lower left), and whole century (lower right).

### 3.6. Isoprene

Higher temperatures and stronger radiation both support the emission of biogenic hydrocarbons. Isoprene and monoterpenes are the only ozone precursors, with changing emissions in the decades calculated in this study. The change of the volume mixing ratio of isoprene is displayed in *Fig. 6*. The upper left panel shows the summer average of isoprene during the control period. Since the lifetime of isoprene amounts to only a few hours or even less, noteworthy concentrations occur over the land areas only. The highest values can be found over Portugal and the Balkan. Until the decade from 2041 to 2050 the values increase slightly over most of the model domain. Even over the sea a small increase is plotted. The increase continues until the end-century decade. During this time span there is a greater increase of the isoprene concentration over the areas that had the highest abundance already.

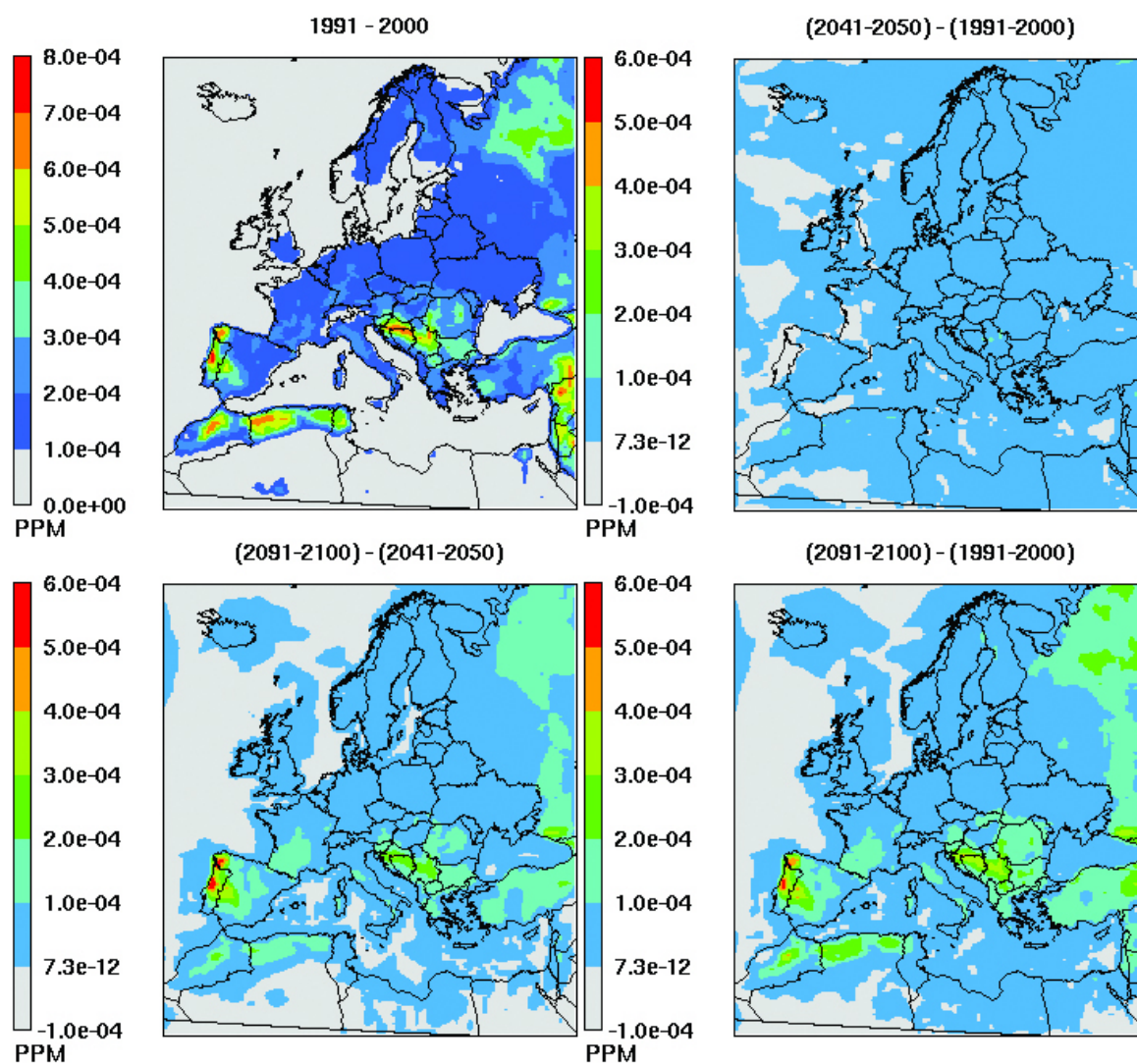


*Fig. 6.* Average volume mixing ratio of isoprene in the lowest model level in summer (JJA) in the control decade 1991–2000 (upper left), and differences of the average volume mixing ratios in summer between the calculated decades: first half-century (upper right), second half-century (lower left), and whole century (lower right).

#### 4. Discussion

Photochemical model calculations, which are driven by meteorological fields from climate scenario runs with a regional climate model, show an increase of ozone formation concurrent with climate change. In the second half of the 21st century, the increase of the ozone concentration is much stronger than in the first half, coinciding with a larger increase in average temperature and a decrease of the average cloud optical depth.

Since ozone is a secondary pollutant that is formed in the atmosphere, its abundance depends on the availability of sufficient ozone precursors. In addition, the right conditions must be present, including the presence of high temperatures, strong solar radiation, and stagnant winds. Biogenic emissions were the only variable ozone precursors in this study, and their emission in turn depends on temperature and radiation in the model. Therefore, it follows that ozone should increase mostly where the highest increases of temperature and radiation occur.

By comparing the results for the decade 2041–2050 with the control period 1991–2000, the changes projected for the first half of the 21st century can be seen. A small increase of temperature occurs over most parts of Europe. On the other hand, there is also an increase in the cloud optical depth, which, therefore, counteracts ozone formation due to less radiation. This results in only a small increase of the averaged daily maxima of ozone in southeastern Europe, where the effect of temperature change seems to outweigh the effect of radiation. In northern and western Europe the opposite occurs and the average daily maxima of ozone are reduced. Similar results of increasing and decreasing values are obtained for AOT40 (Apr–Sep) as well as for other ozone measures, which are not shown.

In the second half of the 21st century, the temperature increase in the input data is much stronger, and the radiation increases due to a decrease of the cloud optical depth. Therefore the calculated increase of ozone in all parts of Europe is also much stronger in the later half of the 21st century

The highest changes of ozone occur in summer, the season that shows the highest ozone concentrations. Interestingly, these future increases in ozone occur where the highest emissions of ozone precursors are present, not where the highest temperature increases occur. From the increase of the averaged daily maxima of ozone it can be concluded, that the ozone concentration would exceed present legal thresholds in the future more often under the assumptions of unchanged anthropogenic emissions of ozone precursors. The long-term objective for AOT40 (Apr–Sep) of 10000 ppbv h will also not be maintained under these conditions.

An increase of biogenic hydrocarbon emissions caused by higher temperatures and stronger radiation certainly supports ozone formation. However, this effect should be treated with caution, since the meteorological effects also may lead to changes in land use, which in turn affects the intensity of emissions. In addition, there are indications that the production of isoprene by

forest ecosystems may be reduced under conditions of elevated CO<sub>2</sub> concentrations (*Rosenstiel et al.*, 2003, *Monson et al.*, 2007), which is the main driving force for the projected climate change. Such feedbacks were not considered in this study and land use patterns were kept constant over all decades.

Furthermore, areas with the strongest increase of biogenic emissions must not be, by all means, the areas with the strongest ozone increase, since NO<sub>x</sub> must also be available for ozone formation. For example, the Balkan area shows a strong increase of isoprene until the 2091–2100 decade (*Fig. 6*), while the increase of ozone in that area is not exceptionally strong (*Fig. 1* and *Fig. 3*). *Forkel and Knoche* (2007) show similar results for this area and explain them with the lack of NO<sub>x</sub>.

The concentration of ozone may also change due to alterations of the patterns of horizontal atmospheric transport within the model domain. Such phenomena have not been investigated in this study. On the other hand, effects of vertical transport were excluded from this study, since constant clean air conditions have been assumed at the top of the model.

The coarse grid resolution of 50 km in the CAMx calculation implies, that this is a study for background concentrations. The highest concentrations of ozone are normally observed within urban plumes, while urban areas, on the other hand, usually show a strong reduction of ozone during nighttime due to destruction by primary emissions of NO. These features are not resolved with the applied model grid. In addition, the 50 km resolution of the used emission inventory causes an instantaneous mixing of emitted ozone precursors. This also prevents the formation of high ozone concentrations as well as local destruction. Therefore, extreme high and low ozone values may not be expected in the model results. Within the project CECILIA, air quality calculation with a higher spatial resolution will be performed at a later stage for smaller model domains.

The results of this study agree well with results from other studies, although they may be compared only qualitatively, since other studies use different greenhouse gas scenarios and different time periods are considered. *Forkel and Knoche* (2007) calculated the 2030s-decade as climate projection, and also found an increase of ozone over Europe. *Hedegaard et al.* (2008) performed their calculations for the same decades as in this study, but they used the A2 scenario and a coarser model resolution. However, they did not find the distinction between small changes in the first half and strong changes in the second half of the 21st century that was found in this work. This difference is likely to be caused by the different GCM boundary conditions. *Meleux et al.* (2007) looked at time slices of 30 years, in contrast to 10 years in the other studies. However, their qualitative result is very similar. Nonetheless, the fact, that different models applied under partly different assumptions lead to qualitatively similar results, shows some robustness of the message that the projected climate change would lead to enhanced ozone formation if anthropogenic emissions would be kept unchanged.

## 5. Summary and conclusions

Regional photochemical model simulations were carried out with the model CAMx. The model domain covered Europe with a spatial resolution of 50 km. Three decades were calculated, namely 1991–2000, 2041–2050, and 2091–2100, driven by a climate change simulation of the model RegCM. These in turn were driven by the global model simulation of the ECHAM5 model under the SRES-A1B-greenhouse gas scenario.

Of the many species calculated by the photochemical model, this study mainly examined ozone concentrations during summer due to its adverse effects on human health and vegetation. Ozone levels are projected to increase over Europe during the 21st century. The increase will be stronger in the second half of the century; in the first half a decrease in northern parts of Europe is projected.

The projected ozone increase must be attributed to more frequent meteorological conditions that promote ozone formation like high temperature, strong solar radiation, and stagnant flow conditions. In addition, increasing concentration of biogenic hydrocarbons calculated with respect to the meteorological input data, which in turn are dependent on the temperature and the available radiation, may also be a factor in the projected ozone increases.

**Acknowledgement**—This work has been funded by the European Community's Sixth Framework Programme as part of the project CECILIA (Central and Eastern Europe Climate Change Impact and Vulnerability Assessment) under Contract No. 037005.

## References

- Chang, J.S., Brost, R.A., Isaksen, I.S.A., Madronich, S., Middleton, P., Stockwell, W.R., and Walcek, C.J., 1987: A three-dimensional Eulerian acid deposition model: Physical concepts and formulation. *J. Geophys. Res.* 92, 14681-14700.
- ENVIRON, 2006: *User's Guide to the Comprehensive Air Quality Model with Extensions (CAMx)*, Version 4.40. ENVIRON International Corporation, Novato, CA.
- European Communities, 2002: Directive 2002/3/EC of the European Parliament and of the Council of 12 February 2002 relating to ozone in ambient air. *Official J. of the European Communities*, L67/14, EN.
- Forkel, R. and Knoche, R., 2007: Nested regional climate-chemistry simulations for central Europe. *C. R. Geoscience* 339, 734-746.
- Gery M.W., Whitten G.Z., Killus, J.P., and Dodge, M.C., 1989: A photochemical kinetics mechanism for urban and regional scale computer modelling. *J. Geophys. Res.* 94, 12925-12956.
- Guenther, A.B., Zimmermann, P.C., Harley, R., Monson, R.K., and Fall, R., 1993: Isoprene and monoterpene emission rate variability: model evaluations and sensitivity analyses. *J. Geophys. Res.* 98, 12609-12617.
- Hedegaard, G.B., Brandt, J., Christensen, J.H., Frohn, L. M., Geels, C., Hansen, M., and Stendel, M., 2008: Impacts of climate change on air pollution levels in the Northern Hemisphere with special focus on Europe and the Arctic. *Atmos. Chem. Phys. Discuss.* 8, 1757-1831.
- Meleux, F., Solmon, F., and Giorgi, F., 2007: Increase in summer European ozone amounts due to climate change. *Atmos. Environ.* 41, 7577-7587.
- Monson, R., Trahan, N., Rosenstiel, T., Veres, P., Moore, D., Wilkinson, M., Norby, R., Volder, A., Tjoelker, M., Briske, D., Karnosky, D., and Fall, R., 2007: Isoprene emission from terrestrial

- ecosystems in response to global change: minding the gap between models and observations. *Philos. T. Roy. Soc.A.* 365, 1677-1695.
- Nakicenovic, N., Alcamo, J., Davis, G., de Vries, B., Fenhann, J., Gaffin, S., Gregory, K., Grübler, A., Jung, T., Kram, T., Rovere, E.L., Michaelis, L., Mori, S., Morita, T., Pepper, W., Pitcher, H., Price, L., Riahi, K., Roehrl, A., Rogner, H.-H., Sankovski, A., Schlesinger, M., Shukla, P., Smith, S., Swart, R., van Rooijen, S., Victor, N., and Dadi, Z., 2000: *Special Report on Emission Scenarios*. Cambridge University Press.
- O'Brien, J.J., 1970: A note on the Vertical Structure of Eddy Exchange Coefficient in the Planetary Boundary Layer. *J. Atmos. Sci.* 27, 1213-1215.
- Pal, J.S., Giorgi, F., Bi, X., Elguindi, N., Solomon, F., Gao, X., Rauscher, S.A., Francisco, R., Zakey, A., Winter, J., Ashfaq, M., Syed, F.S., Bell, J.L., Diffenbaugh, N.S., Karmacharya, J., Konare, A., Martinez, D., da Rocha, R.P., Sloan, L.C., and Steiner, A., 2007: Regional climate modeling for the developing world: The ICTP RegCM3 and RegCNET. *B. Am. Meteorol. Soc.* 88, 1395-1409.
- Rosenstiel, T.N., Potosnak, M.J., Griffin, K.L., Fall, R., and Monson, R.K., 2003: Increased CO<sub>2</sub> uncouples growth from isoprene emission in an agriforest ecosystem. *Nature* 421, 256-259.
- Simpson, D., Fagerli, H., Jonson, J.E., Tsyro, S., Wind, P., and Tuovinen, J.-P., 2003: Transboundary acidification and eutrophication and ground level ozone in Europe: Unified EMEP Model Description. *EMEP Status Report 1/2003 Part I*, EMEP/MSC-W Report, The Norwegian Meteorological Institute, Oslo, Norway.
- Trickl, T., Cooper, O., Eisele, H., James, P., Mücke, R., and Stohl, A., 2003: Intercontinental transport and its influence on the ozone concentrations over central Europe: Three case studies. *J. Geophys. Res.* 108, 8530.
- Uppala, S. M., Källberg, P. W., Simmons, A. J., Andrae, U., da Costa Bechtold, V., Fiorino, M., Gibson, J. K., Haseler, J., Hernandez, A., Kelly, G.A., Li, X., Onogi, K., Saarinen, S., Sokka, N., Allan, R.P., Andersson, E., Arpe, K., Balmaseda, M.A., Beljaars, A.C.M., van de Berg, L., Bidlot, J., Bormann, N., Caires, S., Chevallier, F., Dethof, A., Dragosavac, M., Fisher, M., Fuentes, M., Hagemann, S., Hólm, E., Hoskins, B.J., Isaksen, I., Janssen, P.A.E. M., Jenne, R., McNally, A.P., Mahfouf, J.-F., Morcrette, J.-J., Rayner, N.A., Saunders, R.W., Simon, P., Sterl, A., Trenberth, K.E., Untch, A., Vasiljevic, D., Viterbo, P., and Woollen, J. 2005: The ERA-40 re-analysis. *Q. J. Roy. Meteorol. Soc.* 131, 2961-3012.
- Vestreng, V., Breivik, K., Adams, M., Wagener, A., Goodwin, J., Rozovskaya, O., and Pacyna, J.M., 2005: Inventory Review 2005, Emission Data reported to LRTAP Convention and NEC Directive, Initial review of HMs and POPs. *Technical Report MSC-W 1/2005*, ISSN 0804-2446.
- Williams, E.J., Parrish, D.D., and Fehsenfeld, F.C., 1987: Determination of NO<sub>x</sub> emissions from soils. *J. Geophys. Res.* 92, 2173-2179.
- Winiwarter, W. and Zueger, J., 1996: Pannonisches Ozonprojekt, Teilprojekt Emissionen. Endbericht. Report OEFZS-A-3817, Austrian Research Center, Seibersdorf.